



LABORATORI NAZIONALI DI FRASCATI  
SIS-Pubblicazioni

LNF-97/040(P)

26 Novembre 1997

**DEAR, FINUDA, KLOE:  
Kaonic Atoms, Hypernuclei and CP-Violation  
at the DAΦNE  $\Phi$ -Factory**

Stefano Bianco

*INFN-Laboratori Nazionali di Frascati,  
Via Enrico Fermi 40, 00044 Frascati, Italy*

**Abstract**

Physics at DAΦNE , the new Frascati  $e^+e^-$  machine, is reviewed, as well as the experiments: DEAR - search for  $KN$  exotic atoms, FINUDA - spectroscopy and decays of hypernuclei, and KLOE - a multipurpose detector designed for detecting direct CP violation.

PACS: 13.20.Eb; 13.65.+i; 29.20.Dh; 21.80.+a

Invited Talk Delivered at the II SILAFAE  
November 1996, Merida, Yucatan (Mexico).

## 1 Introduction

The DAΦNE  $e^+e^-$  collider facility <sup>1)</sup>, <sup>2)</sup>, <sup>3)</sup>, proposed in 1990 <sup>4)</sup>, has been completed in mid 1997 at the Laboratori Nazionali di Frascati of INFN, and it is now being commissioned. The DAΦNE collider <sup>5)</sup> <sup>6)</sup> will operate at the center of mass energy of the  $\phi$  meson with an initial luminosity  $\mathcal{L} = 1.3 \times 10^{32} \text{cm}^{-2} \text{s}^{-1}$  and a target luminosity  $\mathcal{L} = 5.2 \times 10^{32} \text{cm}^{-2} \text{s}^{-1}$ .

The  $\phi(1020)$  meson <sup>1</sup> is produced in  $e^+e^-$  collisions with a

$$\sigma(e^+e^- \rightarrow \phi) = 4.4 \mu\text{b}$$

peak cross section, which translates into a production rate of

$$R_\phi = 2.3 \times 10^3 \text{s}^{-1}$$

at target luminosity. The production cross section  $\sigma(e^+e^- \rightarrow \phi)$  should be compared with the hadronic production which, in this energy range, is given by

$$\sigma(e^+e^- \rightarrow f\bar{f}) = \frac{4\pi\alpha^2}{3s} Q_f^2 = \frac{86.8 Q_f^2 \text{nb}}{s[\text{GeV}^2]} = 56 \text{nb},$$

i.e., with an integral S/N ratio of about 40:1.

The  $\phi$  then decays at rest into  $K^+K^-$  (49%),  $K^0\bar{K}^0$  (34%),  $\rho\pi$  (13%),  $\pi^+\pi^-\pi^0$  (2.5%) and  $\eta\gamma$  (1.3%), which translate in 0.8 kHz  $\phi \rightarrow K^0\bar{K}^0$ , 1.1 kHz  $\phi \rightarrow K^+K^-$ , 300 Hz  $\phi \rightarrow \rho\pi$ , 60 Hz  $\phi \rightarrow \pi^+\pi^-\pi^0$ , 30 Hz  $\phi \rightarrow \eta\gamma$ . With a canonical efficiency of 30%, this corresponds to  $2 \times 10^{10}$   $\phi$  decays in one calendar year. Therefore, a  $\phi$ -factory is a unique source of monochromatic (110 and 127 MeV/c, respectively), slow <sup>2</sup>, collinear, quantum-defined (pure  $J^{PC} = 1^{--}$  quantum states), and tagged <sup>3</sup> neutral and charged kaons.

With  $\mathcal{O}(10^{10})$  kaons per year we can form kaonic atoms and study K-Nucleon interactions at low energy (DEAR), produce nuclei with strangeness (*hypernuclei*, FINUDA), and study particle physics fundamental symmetries (KLOE).

---

<sup>1</sup> Quantum numbers and physical constants for the  $\phi(1020)$  meson are:  $s\bar{s}$  quark assignment, mass  $m = 1019.413 \pm 0.008 \text{ MeV}$ , total width  $\Gamma = 4.43 \pm 0.06 \text{ MeV}$ , electronic width  $\Gamma_{ee} = 1.37 \pm 0.05 \text{ keV}$ , and  $I^G(J^{PC}) = 0^-(1^{--})$  quantum numbers.

<sup>2</sup> Kaons are produced with  $\beta_K \simeq 0.2$ . Therefore they travel a short path before decaying, and can be stopped after crossing very little matter. Experimentally, this translates into small detectors and thin targets.

<sup>3</sup>The detection of one K out of the two produced in the  $\phi$  decay determines the existence and direction of the other K.

Table 1: Quantum number assignments for kaons.

	$I_3 = +1/2$	$I_3 = -1/2$
$S = +1$	$K^+(s\bar{u})$	$K^0(\bar{s}d)$
$S = -1$	$\bar{K}^0(s\bar{d})$	$K^-(s\bar{u})$

## 2 A brief history of kaons

The kaonic enigma <sup>7), 8)</sup> began in 1947 with their very discovery in p-N interactions such as  $\pi^- + p \rightarrow \Lambda + K^0$ . The long lifetime  $\sim 10^{-10}$ s, and the fact they were always produced in pairs, was explained by postulating a new quantum number *strangeness* conserved by strong interactions (production) but not weak interactions (decay) (Tab.1). In 1956, Lee and Yang postulated first, and Wu et al. demonstrated next (1957), that the  $\tau - \theta$  puzzle [the same  $K^+$  particle decaying to opposite parity ( $2\pi, 3\pi$ ) states] was actually caused by P and C being violated in weak decays, with CP conserved. In 1964 Christenson, Cronin, Fitch and Turlay disproved this hypothesis by studying  $K^0$  decays.  $K^0$  and  $\bar{K}^0$  have same quantum numbers except S, which is not conserved in weak interactions; therefore, they have common virtual decay channels and they can oscillate when decaying <sup>4)</sup>:

$$K^0 \leftrightarrow 2\pi (CP = +1) \leftrightarrow \bar{K}^0 \quad K^0 \leftrightarrow 3\pi (CP = -1) \leftrightarrow \bar{K}^0$$

with the CP eigenstates being

$$|K_{1,2}^0\rangle = (|K^0\rangle \pm |\bar{K}^0\rangle)/\sqrt{2}$$

and time evolution

$$P(K^0, t) = 1/4[e^{-\Gamma_1 t} + e^{-\Gamma_2 t} - 2e^{-(\Gamma_1 + \Gamma_2)t/2} \cos \Delta m t].$$

The decay of neutral kaons to pions is Cabibbo-unfavoured: since the phase space available for  $2\pi$  is much greater than for  $3\pi$ , lifetimes will be largely different  $\Gamma_1 \gg \Gamma_2$ . Quite fortuitously, the oscillation frequency is  $\Delta m \equiv |m_1 - m_2|$ , large and observable, since the mass difference is comparable to the width of the short-lived state  $\frac{\Delta m}{\Gamma_1} \sim 0.5$ . Christenson et al. indeed showed that a  $10^{-3}$  fraction of  $K_2$ 's decay to  $2\pi$ . Physical states are therefore

$$|K_L\rangle \propto |K_2\rangle + \epsilon|K_1\rangle \quad \text{and} \quad |K_S\rangle \propto \epsilon|K_2\rangle + |K_1\rangle.$$

The  $\epsilon$  parameter describes *indirect* CP violation (CPV in short), which originates from the mass matrix mixing ( $\Delta S = 2$  transitions), not from the interaction responsible of the decay.

---

<sup>4)</sup>The  $3\pi$  state has  $CP = -1$  when in the L=0 state, with the L=1 state being depressed by centrifugal potential.

The central role played by the  $K^0 - \bar{K}^0$  mixing was revived in 1970. The suppressed nature of neutral-current decays such as  $K_L^0 \rightarrow \mu\mu$  was explained through GIM-like box-diagrams and predicted a fourth flavour - *charm* - with mass  $m_C^2 \propto \Delta m$ .

Together with CPV from mixing, there can be a *direct* ( $\Delta S = 1$ ) transition from  $|K_L(CP = -1)\rangle$  to  $|2\pi(CP = +1)\rangle$ , without  $K^0 \leftrightarrow \bar{K}^0$  intermediate transition. Direct CPV is parametrized by

$$\epsilon' \propto \frac{\langle 2\pi I = 2 | H | K^0 \rangle}{\langle 2\pi I = 0 | H | K^0 \rangle}.$$

The issue of CPV is a most fundamental one. As first emphasized by Sakharov in 1967, the predominant asymmetry of baryons versus antibaryons in the universe could be explained by three requirements: baryon number non-conservation, a CPV baryon-creating process, with baryons out of the thermal equilibrium. See M. Gleiser's talk at this Symposium <sup>9)</sup>.

Models proposed so far can be schematically distinguished in two classes, milliweak and superweak. Milliweak models advocate that a tiny ( $10^{-3}$ ) fraction of the weak interaction is indeed CPV at leading order ( $\Delta S = 1$ ). They imply T violation to guarantee the CPT theorem, and they can explain both direct [one ( $\Delta S = 1$ ) transition] and indirect [two ( $\Delta S = 1$ ) transitions]. Superweak models (Wolfenstein, 1964), on the other hand, postulate a new ( $\Delta S = 2$ ), CPV process which transforms  $K_L \rightarrow K_S$ . The strength of this interaction relative to weak coupling is only  $10^{-10}$ , since  $M_{K_S} \simeq M_{K_L}$  and, therefore, no direct CPV is predicted nor allowed, no CPV is expected in other systems. The standard model (SM), a milliweak-type theory, *naturally* allows for CPV: the angle  $\delta$  in the CKM matrix allows for CPV transitions

$$V_{CKM} = \begin{pmatrix} 1 - \lambda^2/2 & \lambda & A\lambda^3\sigma e^{-i\delta} \\ \lambda & 1 - \lambda^2/2 & A\lambda^2 \\ A\lambda^3(1 - \sigma e^{i\delta}) & -A\lambda^2 & 1 \end{pmatrix} + \mathcal{O}(\lambda^3) \quad (1)$$

where  $\lambda \equiv \sin \theta_C$ ,  $\rho - i\eta \equiv \sigma e^{-i\delta}$ .

The indirect CPV parameter  $\epsilon$  is proportional in the SM picture to  $\Delta S = 2$  box diagrams (Fig.1a)  $\epsilon \propto \lambda^4 \sin \delta \simeq 10^{-3} \sin \delta$ . Therefore,  $\epsilon$  is small per se because of the suppression of interfamily transitions, while the CPV angle  $\delta$  is not necessarily small. Experimentally,  $|\epsilon| = 2.26(2) \times 10^{-3}$ .

The direct CPV parameter  $\epsilon'$ , on the other hand, is proportional in the SM picture to  $\Delta S = 1$  *penguin* diagrams (Fig.1b) which are difficult to compute, and suppressed by both the  $\Delta I = 1/2$  and the Zweig rule <sup>5</sup>. Calculations <sup>13)</sup> have shown how in the

<sup>5</sup>We do not discuss here the third piece of experimental information that can be used to set limits to the CPV angle  $\delta$ , i.e. the experimental bounds on the electric dipole moments of the neutron and the electron. See <sup>10)</sup> and references therein for a thorough review.

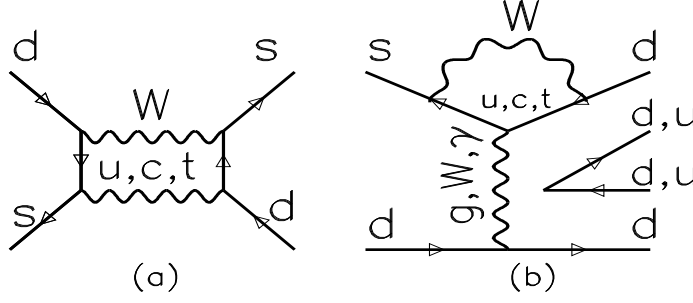


Figure 1: a)  $K^0 - \bar{K}^0$  mixing b) Direct CP violation through *penguin* diagrams.

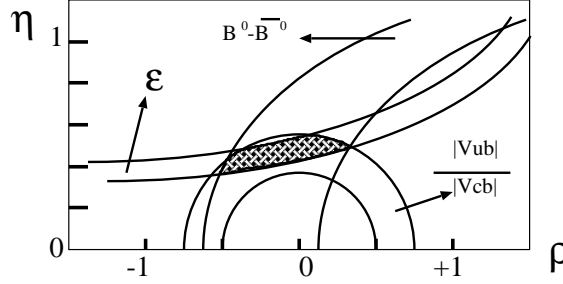


Figure 2: Qualitative sketch showing bounds on the CP violating angle of CKM matrix.

SM picture direct CPV is a decreasing function of the quark masses in the penguin loop, primarily the top quark mass. Prediction for  $m_{top} = 175$  GeV is  $0 \leq \epsilon'/\epsilon \leq 0.001$ .

One can try and use the precise measurement of  $|\epsilon|$  to set bounds on  $\delta$ , although along with the use of the experimental values from the  $B_d^0 - \bar{B}_d^0$  mixing and the ratio of CKM elements  $|V_{ub}|/|V_{cb}|$ , obtaining <sup>10)</sup> the qualitative picture in Fig.2.

Finally, the most precise measurements <sup>6</sup> of the relative strength of direct versus indirect CPV yield result in mild agreement:  $\Re(\epsilon'/\epsilon) = (7.4 \pm 5.2 \pm 2.9) \times 10^{-4}$  (E731 at Fermilab <sup>11)</sup>) and  $\Re(\epsilon'/\epsilon) = (23.0 \pm 3.6 \pm 5.4) \times 10^{-4}$  (NA31 at CERN <sup>12)</sup>) as measured from the double-ratio <sup>7</sup>

$$\left| \frac{\eta_{+-}}{\eta_{00}} \right|^2 = \frac{N(K_L \rightarrow \pi^+\pi^-)/N(K_S \rightarrow \pi^+\pi^-)}{N(K_L \rightarrow \pi^0\pi^0)/N(K_S \rightarrow \pi^0\pi^0)} \simeq 1 + 6\Re(\epsilon'/\epsilon) \quad (2)$$

From the body of information available, the CPV angle  $\delta$  seems to be large ( $\rho \simeq 0 \Rightarrow \delta \simeq \pi/2$ ); a large top mass (175 GeV) predicts  $\Re(\epsilon'/\epsilon)$  to be in the  $10^{-4}$  region <sup>13)</sup>; a measurement of  $\Re(\epsilon'/\epsilon) \neq 0$  will indicate the general validity of the CKM picture, since it requires the presence of a  $\Delta S = 1$  phase.

<sup>6</sup> Experimentally,  $|\eta_{+-}| \simeq |\eta_{00}| \simeq 2 \times 10^{-3}$  and  $\phi_{+-} \simeq \phi_{00} \simeq 44^\circ$ . Therefore,  $\epsilon'/\epsilon \simeq \Re(\epsilon'/\epsilon)$ .

<sup>7</sup>The following useful relationships also hold:

$$\eta_{+-} \equiv \epsilon + \epsilon' \equiv \frac{\langle \pi^+\pi^- | H | K_L \rangle}{\langle \pi^+\pi^- | H | K_S \rangle} \quad \eta_{00} \equiv \epsilon - 2\epsilon' \equiv \frac{\langle \pi^0\pi^0 | H | K_L \rangle}{\langle \pi^0\pi^0 | H | K_S \rangle}.$$

### 3 KLOE

The KLOE experiment was proposed in April 1992; approved and funded at the beginning of 1993, construction of the detector began in 1994. The principal aim of KLOE is the detection of direct CP violation in  $K^0$  decays with a  $10^{-4}$  sensitivity on  $\Re(\epsilon'/\epsilon)$ . For a comprehensive review see <sup>14)</sup> and references therein, while an up-to-date status report can be found in <sup>15)</sup>. The measurement in KLOE of  $\Re(\epsilon'/\epsilon)$  with the required precision takes advantage of unique features of a  $\phi$ -factory: numerous kinematical constraints exist,  $K_S$  and  $K_L$  are detected at the same time, clean environment typical of  $e^+e^-$  machines with respect to experiments at extracted hadron beams, built-in calibration processes. On the down side, the  $K_S$  and  $K_L$  are detected with different topologies in both the charged and the neutral decay modes.

KLOE should be regarded as a precision kaon interferometer. As already stressed, collinear kaon pairs are produced from the  $\phi$  decay in a pure, coherent quantum state. If one of the two neutral kaons from the  $\phi$  decays into a state  $f_1$  at time  $t_1$  and the other to a state  $f_2$  at time  $t_2$ , the decay intensity to  $f_1$  and  $f_2$  as a function of  $\Delta t \equiv t_1 - t_2$  is

$$I(f_1, f_2; \Delta t; \forall \Delta t > 0) = \frac{1}{2\Gamma} |\langle f_1 | K_S \rangle \langle f_2 | K_S \rangle|^2 [|\eta_1|^2 e^{-\Gamma_L \Delta t} + |\eta_2|^2 e^{-\Gamma_S \Delta t} - 2|\eta_1||\eta_2| e^{-\Gamma \Delta t/2} \cos(\Delta m \Delta t + \phi_1 - \phi_2)] \quad (3)$$

where  $\eta_i \equiv \langle f_i | K_L \rangle / \langle f_i | K_S \rangle$ , and  $\Gamma \equiv (\Gamma_S + \Gamma_L)/2$ . The interference term in the decay intensities above gives measurements of all sixteen parameters describing CP and CPT (if any) violations in the neutral kaon system <sup>10)</sup>. As instance, when  $f_1 = f_2$ , one measures  $\Gamma_S, \Gamma_L$  and  $\Delta m$ ; when  $f_1 = \pi^+\pi^-, f_2 = \pi^0\pi^0$ , one measures  $\Re(\epsilon'/\epsilon)$  at large  $\Delta t$ , and  $\Im(\epsilon'/\epsilon)$  near  $\Delta t = 0$ .

Other physics topics include rare  $K_S^0$  decays ( $10^{10}$  kaons per year will improve the sensitivity to branching ratios down to the  $10^{-8}$  range), tests of Chiral Perturbation Theories, radiative  $\phi$  decays, and  $\gamma\gamma$  physics <sup>16)</sup>. Out of such a physics spectrum other than CPV, it should be underlined the importance of a study of the  $J^{PC} = 0^{++} f_0(975)$  meson state, produced via the  $\phi$  radiative decay with a branching ratio at least  $1 \times 10^{-6}$ . The nature of the lightest scalar is still unclear, whether a  $KK$  molecule, an exotic  $qq\bar{q}\bar{q}$  or a glue-ball state. The decay  $f_0 \rightarrow \pi^0\pi^0$  should be easily measured even at low luminosity during the machine commissioning <sup>17)</sup>, while the charged channel  $\pi^+\pi^-$  suffers by backgrounds from continuum.

To reach the design sensitivity on the measurement of  $\Re(\epsilon'/\epsilon)$  via the classical double-ratio method (Eq.2), a one-year statistics at full DAΦNE luminosity is necessary. It is also necessary to control the detector efficiency for the decays of interest and to reject backgrounds from the copious  $K_L^0$  decays to states other than two-pion.

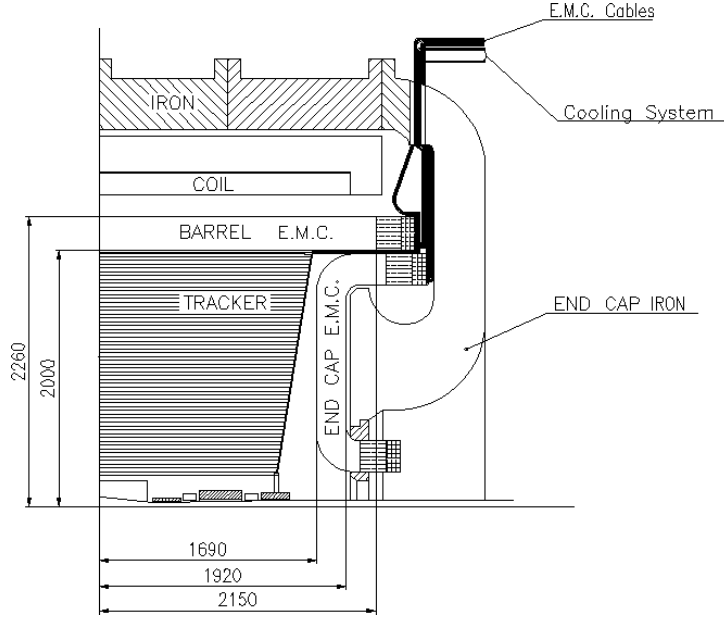


Figure 3: Cross-sectional schematics of the KLOE detector (one quadrant, side view). Dimensions are millimeters.

The KLOE detector <sup>18)</sup> (Fig.3) is a hermetic,  $4\pi$  geometry apparatus: a cylindrical structure surrounding the beam pipe and consisting of a large drift chamber, and an electromagnetic calorimeter with state-of-the-art energy and time resolution <sup>19), 20), 21)</sup>, and a 6 kG superconducting magnet. Counting of the four  $K_S, K_L$  decays used in the double-ratio formula (eq.2) is performed by defining a  $K_S$  fiducial volume (10 cm radius around the interaction point, about 17 lifetimes), and a  $K_L$  fiducial volume (145 cm, about one half lifetime). It is very important to avoid systematical errors in the determination of the boundaries of the fiducial volumes for neutral and charged decay channels. This is accomplished by using  $K_L$  decays where both the neutral and the charged vertex are measured, as in  $K_L \rightarrow \pi^+\pi^-\pi^0$ .

The KLOE calorimeter will reconstruct the  $\pi^0\pi^0$  mode, determine the decay vertex space location, reject the  $3\pi^0$  decay, and provide  $\pi/\mu$  rejection. The technique employed is a Pb-scintillator sampling with 1-mm scintillating fibers embedded in very thin Pb grooved foils, which has been demonstrated to provide good energy ( $\sigma_E/E \simeq 4\%/\sqrt{E[\text{GeV}]}$ ) and space ( $\sigma_{x,y} \simeq 0.5 \text{ cm}/\sqrt{E}$ ,  $\sigma_z \simeq 2 \text{ cm}$ ) resolution, acceptable efficiency for photon energies down to 20 MeV, and spectacular time resolution ( $\sigma_t = 55 \text{ ps}/\sqrt{E[\text{GeV}]}$ ). The measurement of the time of arrival  $t_\gamma$  and the impact point  $(x, y, z)$  at the calorimeter of one photon out of four, and the knowledge of the  $K_S$  flight direction ( $\cos\theta$ ), gives the  $K_L$  decay length  $L_K$  to an accuracy of 1 cm via the formulae

$$t_\gamma = L_K/(\beta_K c) + L_\gamma/c \quad (4)$$

$$L_\gamma^2 = D^2 + L_K^2 - 2DL_K \cos \theta \quad (5)$$

where  $D^2 \equiv x^2 + y^2 + z^2$ .

A He-based, very transparent, drift chamber will reconstruct the  $\pi^+\pi^-$  final state, reject the  $K_{\ell 3}$  background, and determine the  $K_S^0$  flight direction and the charged decay vertices. The KLOE drift chamber has space resolution  $\sigma_{\rho,\phi} = 200 \mu\text{m}$  and  $\sigma_z = 3 \text{ mm}$ , and a 0.5% relative resolution on the transverse momentum.

To achieve the required statistical sensitivity, the entire  $\phi$  event rate (5 kHz) has to be written on tape. The calorimeter will provide triggering for most of the decay channels of interest. The rejection of three neutral-pion decays relies on the calorimeter's hermiticity and efficiency for photons down to 20 MeV energy. The rejection of the  $K_{\mu 3}$  decay over the  $\pi^+\pi^-$  decay of interest is based on several kinematical variables and constraints. The high-resolution features of the tracking limits the residual contamination to  $4.5 \times 10^{-4}$ , at a 6 kG solenoidal field, with a 99.8%  $\pi^+\pi^-$  efficiency.

KLOE expects to be operational at beginning of 1998 <sup>22)</sup>.

#### 4 FINUDA

Nuclear physics topics will be investigated by the FINUDA (standing for *F*isica *N*ucleare a *D*AΦ*n*e) experiment. A nuclear physics experiment carried out at an  $e^+e^-$  collider sounds contradictory in itself, but this is where the uniqueness of the idea lies <sup>23)</sup>: charged kaons from  $\phi$  decays are used as a monochromatic, slow (127 MeV/c), tagged, background-free, high-counting rate beam on a thin target surrounding the beam pipe. The possibility of stopping low-momentum monochromatic  $K^-$  with a thin target (typically  $0.5 \text{ g cm}^{-2}$  of  $^{12}\text{C}$ ) is unique to DAΦNE :  $K^-$ 's can be stopped with minimal straggling very near the target surface, so that outgoing prompt pions do not cross any significant amount of the target and do not undergo any momentum degradation. This feature provides unprecedented momentum resolution as long as very transparent detectors are employed before and after the target.

The FINUDA detector is optimized to perform high-resolution studies of hypernucleus production and non-mesonic decays <sup>24)</sup>, by means of a spectrometer with the large acceptance typical of collider experiments.

Negative kaons stopping inside the target produce a  $Y$ -hypernucleus ( $Y = \Lambda, \Sigma, \dots$ ) via the process

$$K_{stop}^- + {}^A Z \rightarrow {}^A_Y Z + \pi^-, \quad (6)$$

where the momentum of the outgoing  $\pi^-$  is directly related to the level of the hypernucleus formed (two-body reaction). In the case of  $\Lambda$  hypernucleus formation, the following



weak-interaction 'decays' are strongly favored in medium-heavy nuclei

$$\Lambda + n \rightarrow n + n \quad \Lambda + p \rightarrow n + p,$$

with the nucleus undergoing the reactions

$${}^A_{\Lambda}Z \rightarrow ({}^{A-2})Z + n + n \quad {}^A_{\Lambda}Z \rightarrow ({}^{A-2})(Z - 1) + n + p,$$

which are interesting for studying the validity of the  $\Delta I = 1/2$  rule <sup>24)</sup>.

Hypernuclei are a unique playground for both nuclear and particle physics <sup>25)</sup>. A  $\Lambda$  embedded in a nucleus can occupy, because of the strangeness content, levels forbidden to a  $p$  and a  $n$  by the Pauli exclusion principle. Furthermore, the  $I = 0$  assignment makes the  $\Lambda N$  interaction much weaker than the ordinary  $NN$  interaction. In the shell model of nuclei the quarks are confined in bags inside baryons. Baryons inside nuclei maintain their identity and interact by the exchange of mesons. At short distance the bags can fuse, quarks can get deconfined and begin interacting by exchanging gluons. For a  ${}^5_{\Lambda}He$  hypernucleus the two models give different predictions: while in the baryon model the  $\Lambda$  occupies the  $S_{\frac{1}{2}}$  orbital due to its strangeness quantum number, in the quark model the  $u$  and  $d$  quarks inside the  $\Lambda$  cannot stay in the  $S_{\frac{1}{2}}$  but are obliged to move to the  $P_{\frac{3}{2}}$  orbital by Pauli blocking. As a result, different binding energies are predicted by the models.

Besides studies on hypernucleus spectroscopy, interest exists for K-N interactions at low energy <sup>26)</sup>. Recently, the possibility of improving the precision on the  $K_{e2}$  branching ratio by a factor of 3 over the present world average was also discussed <sup>27)</sup>.

FINUDA <sup>28)</sup> is a magnetic spectrometer with cylindrical geometry, optimized in order to have large solid-angle acceptance, optimal momentum resolution (of the order of 0.3 % FWHM on prompt pions) and good triggering capabilities. The geometrical acceptance is 100% in the  $\phi$  angle (which reduces to 80% due to dead material), and approximately  $135^\circ \leq \vartheta \leq 45^\circ$ , thus naturally rejecting  $e^+e^-$  background from Bhabha scattering. FINUDA consists of (Fig.4) an interaction/target region, external tracker, outer scintillator array, and superconducting solenoid.

The  $(K^+, K^-)$  pairs from  $\phi$  decay emerge from the interaction region (Fig.4), and are identified for triggering by exploiting the back-to-back event topology and by identification through  $-(dE/dx)$  in the TOFINO triggering scintillator array. Before impinging on the target, a Si- $\mu$ strip array measure the  $(K^+, K^-)$  coordinates before the nuclear target with  $\sigma \sim 30 - 50 \mu\text{m}$  and provides particle identification by  $-(dE/dx)$ . The monochromatic  $K^-$  is stopped inside the thin target, reaction products are emitted isotropically: the momentum of the prompt pion is proportional to the energy of the hypernuclear level formed, and it is measured by Si- $\mu$ strip, low-mass drift chambers <sup>30)</sup>, and straw tube

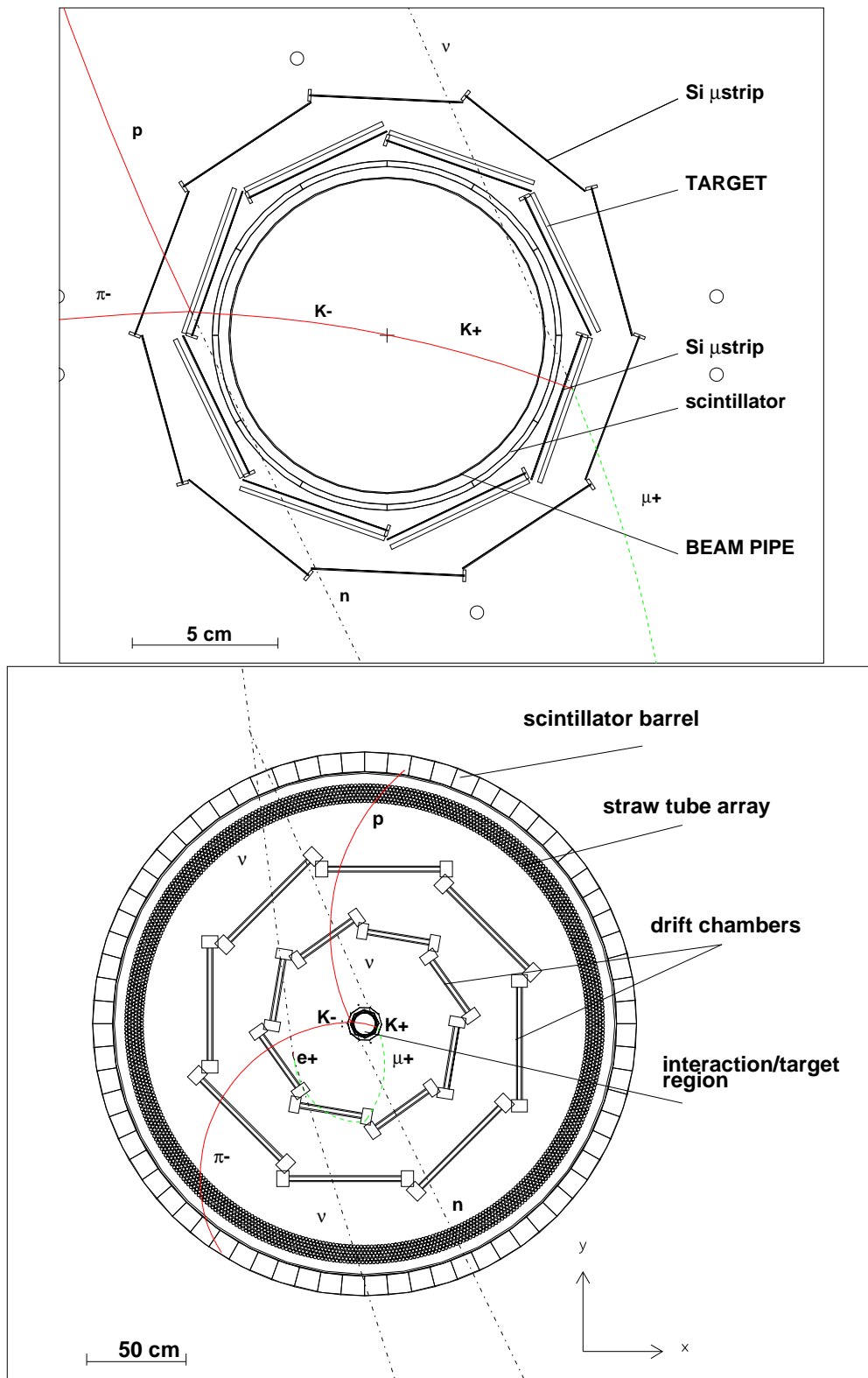


Figure 4: Sketch of the FINUDA detector front (beam) view. The interaction-target region (top); the outer tracker and scintillator barrel (bottom). An hypernuclear event is superimposed. A  $\phi$  decays to  $K^+K^-$ . The  $K^+$  decays to  $\mu^+\nu_\mu$ , followed by  $\mu^+ \rightarrow e^+\nu_e\bar{\nu}_\mu$ . The  $K^-$  crosses the inner trigger scintillator, is tracked by the inner Si- $\mu$ strip detector, stops in the target and forms an hypernucleus (eq.6). The momentum of the emitted prompt  $\pi^-$ , proportional to the energy of the hypernuclear level formed, is measured by the spectrometer. The hypernuclear  $\Lambda$  undergoes the process  $\Lambda p \rightarrow n p$ .

arrays <sup>31)</sup>. The signal in the outer scintillator array (TOFONE) provides a fast trigger logic coincidence. Baryons or mesons from  $\Lambda$  decays are also tracked in the spectrometer (protons,  $\pi^\pm$ ) or detected in the TOFONE (neutrons). The expected FWHM resolution on the 270 MeV/c prompt pion is 0.25% for forward pions (i.e., those emitted towards the outer region of the spectrometer), which corresponds to a 0.7 MeV resolution on the hypernuclear level, to be compared to the best result achieved so far at fixed-target of about 2 MeV <sup>32)</sup>.

The rate of reconstructed hypernuclear events with resolution better than 1 MeV at  $\mathcal{L} = 10^{32} \text{cm}^{-2} \text{s}^{-1}$  is given by the expression:

$$R(\Lambda Z) = R_\phi \times B_{K^+K^-} \times \frac{N_{\Lambda Z}}{K_{stop}} \times \epsilon_{\pi^-} \times \epsilon_{transp} \simeq 2.8 \times 10^{-2} \text{s}^{-1} \simeq 100 \text{ evnts/hr}$$

where  $R_\phi = 5 \times 10^2 \text{s}^{-1}$ ,  $B(\phi \rightarrow K^+K^-) = 0.49$ ,  $N_{\Lambda Z}/K_{stop} = 10^{-3}$  is the capture rate,  $\epsilon_{\pi^-} = 13\%$  is the total efficiency for forward (high-resolution) prompt pions, and  $\epsilon_{transp} = 80\%$  is the chamber transparency.

Superior momentum resolution, high statistics, and low background, make FINUDA capable of resolving hypernuclear states produced at a relative rate of order  $\frac{N_{\Lambda Z}}{K_{stop}} = 10^{-4}$  as simulated in Fig.5 (from ref. <sup>33)</sup>).

The FINUDA experiment expects to be operational by beginning of 1998.

## 5 DEAR

The DEAR experiment <sup>34) 35)</sup> will measure the  $KN$  scattering lengths by studying the shift and the width of the energy levels of kaonic hydrogen and kaonic deuterium atoms, i.e. atoms in which a  $K^-$  from the  $\phi$  decay replaces the orbital electron in a hydrogen, or deuterium, target. The negative kaon then cascades, initially through Auger transitions, and finally through emission of X-rays, whose energy is measured by an array of Charge-Coupled Devices (Fig.7).

The strong interaction between the captured  $K^-$  and the target nucleus shift the energy level of the lowest-lying atomic orbital from their purely em level. Furthermore, the absorption process reduces the state lifetime, thus broadening the width of the X-ray transition.

In the case of kaonic hydrogen, the scattering length  $a_{K^-p}$  is computed from the shift  $\Delta E \equiv E_{exp} - E_{em}$  of the ground level from its computed em value, and the measured width  $\Gamma$  of the X-ray line, via the Deser formula

$$\Delta E + \frac{i\Gamma}{2} = c_{K^-p} a_{K^-p} \quad (7)$$

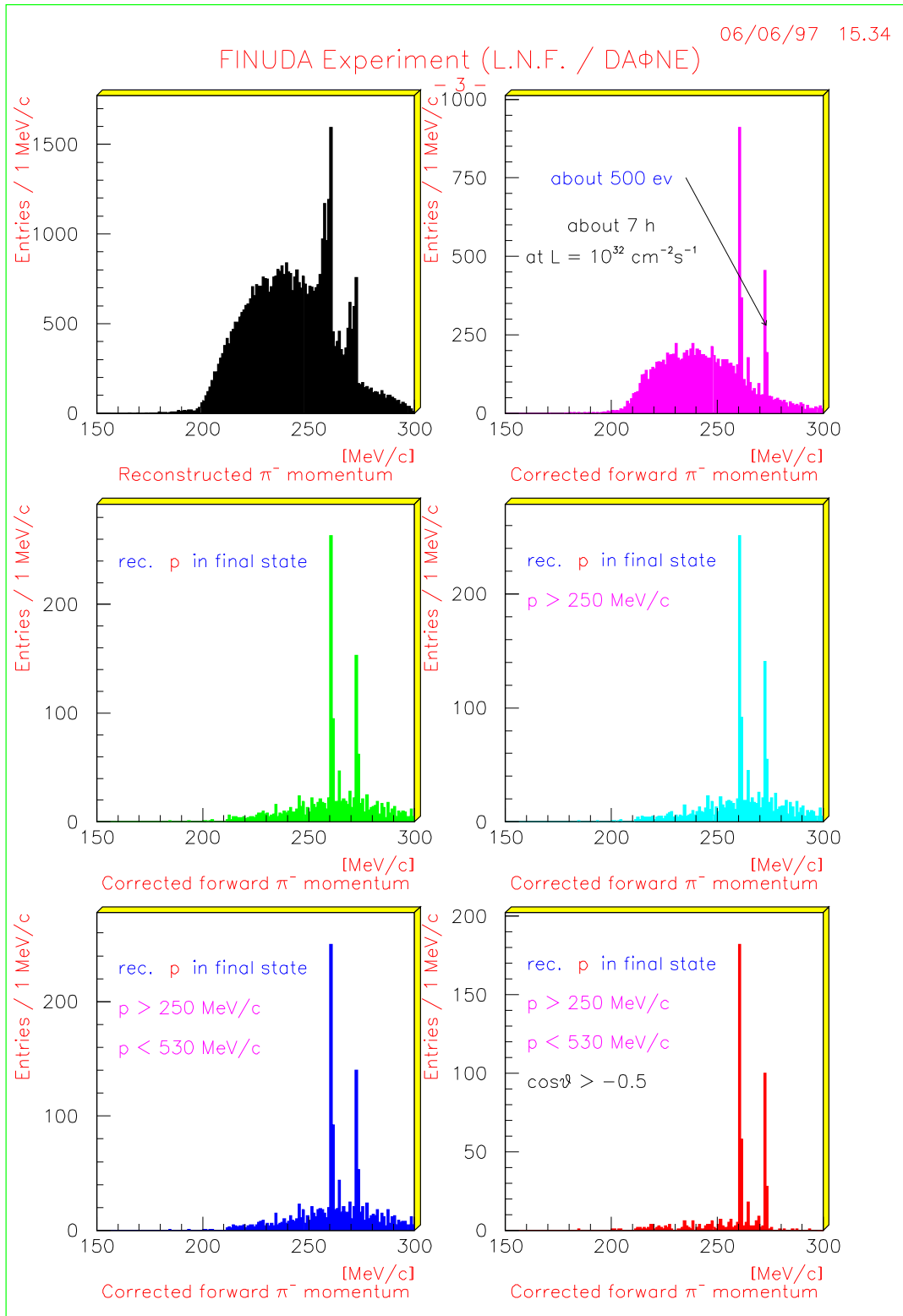


Figure 5: The effect of increasingly stringent cuts on a four-state simulated hypernuclear spectrum, as reconstructed by the FINUDA spectrometer.

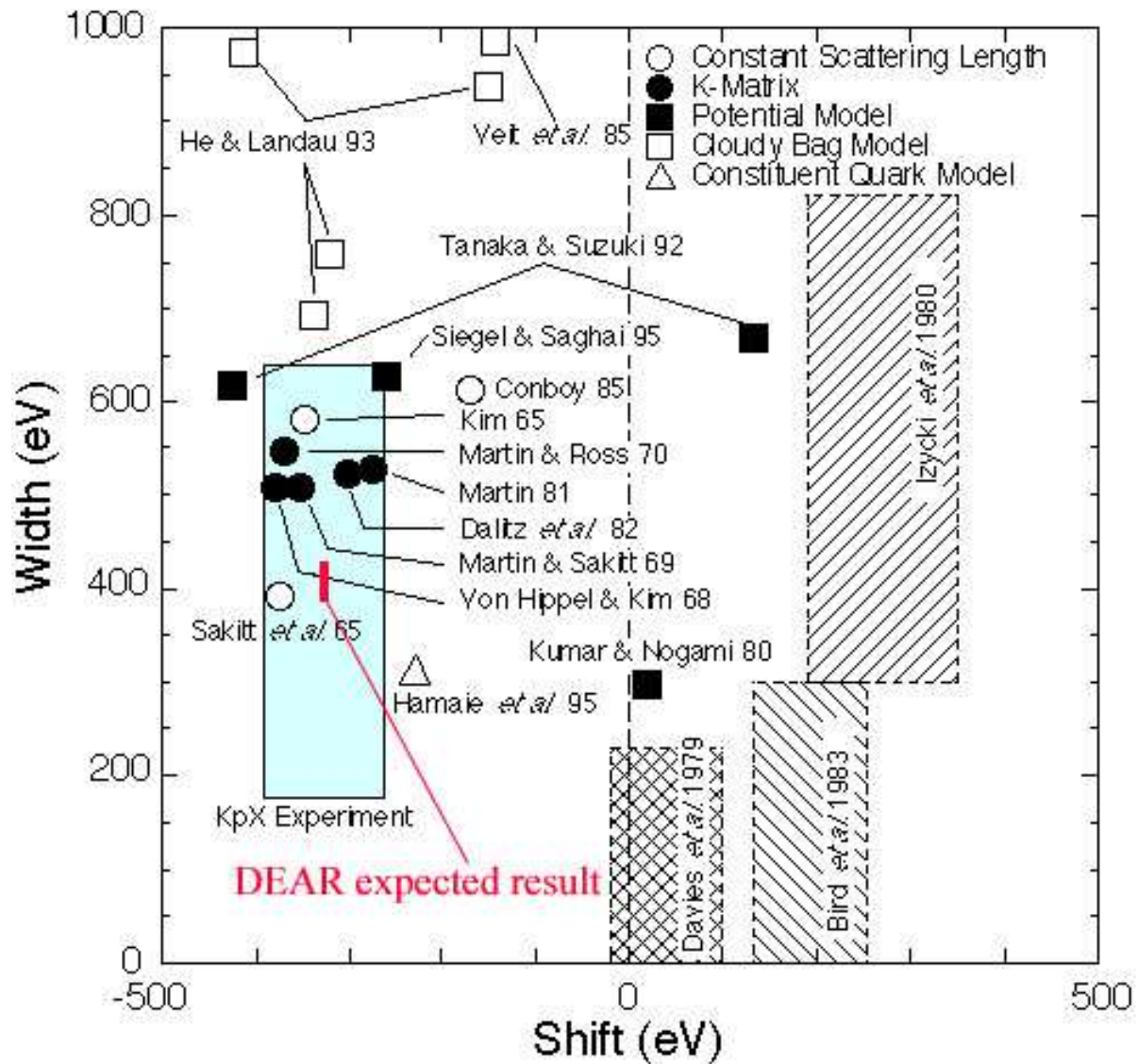


Figure 6: Synopsis of theoretical predictions, experimental results, and simulated DEAR results for shift  $\Delta E$  and width  $\Gamma$  of the  $K_\alpha$  line of kaonic hydrogen.

# DEAR experimental set-up

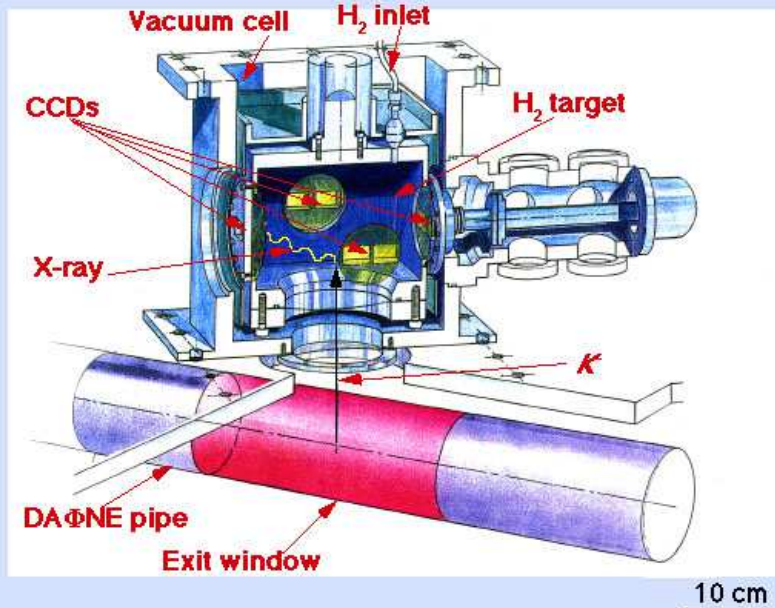


Figure 7: Cut-out sketch of the DEAR setup.

where  $c_{K-p} \equiv \alpha_S^3 \mu^2$ ,  $\alpha_S$  is the strong-interaction fine-structure constant, and  $\mu$  the reduced mass. The (unshifted) em energy levels are computed with a precision of about 1 eV, while the experimental systematics in the detector is at the level of a few eV's.

Experiments performed in the past are mutually inconsistent and disagree with the analysis of low-energy scattering data, whilst recent results from KEK <sup>36)</sup> do confirm the extrapolation at threshold of scattering results (Fig.6).

A detailed simulation of signal and backgrounds, based on a version of the GEANT3 code upgraded to treat photon energies down to 1 keV <sup>37)</sup>, shows that both machine and physical background can be kept under control (Fig.8) with the DEAR setup: the prominent  $K_\alpha$  peak shown (about 10,000 events) can be accumulated with an integrated luminosity of about 500 pb<sup>-1</sup> (ref. <sup>38)</sup>). Superior energy resolution, and lesser background with respect to the KEK experiment, will dramatically reduce the error on the measurements of both shift and width of the  $K_\alpha$  line in kaonic hydrogen, whilst the kaonic deuterium will be measured for the first time (Fig.6).

In addition to the precise determination of low-energy parameters, it has been recently pointed out <sup>38)</sup> how DEAR is able to determine with good precision the so-called KN sigma term ( $\sigma_{KN}$ ). The sigma-term is a quantity which gives indication of the chiral-

## Calculated final DEAR spectrum

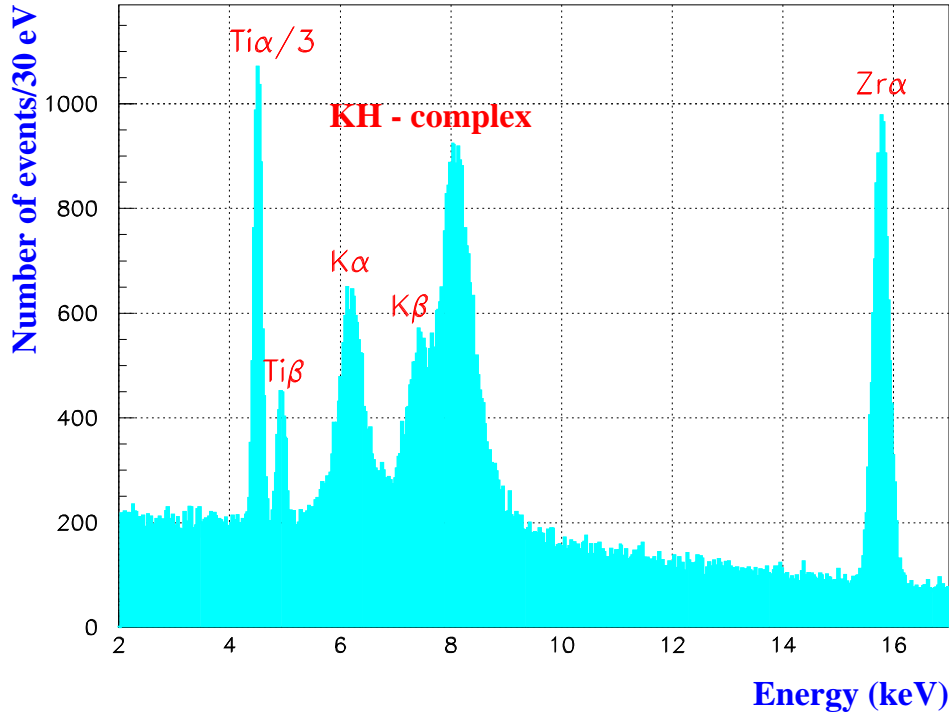


Figure 8: Simulated DEAR spectrum showing the  $K_{\alpha}$ ,  $K_{\beta}$  lines and the  $K_{>\beta}$  complex, along with the  $Ti$  and  $Zr$  calibration lines.

simmetry breaking terms in the strong Hamiltonian <sup>39)</sup>. The theoretical evaluation of the sigma-term requires that the limit of zero-mass pseudoscalar mesons is taken, and therefore approximations are required in order to use experimental data obtained from physical particle processes <sup>40), 41)</sup>. Theoretical studies suggest that  $\sigma_{KN}$  terms be much more sensitive to the  $s\bar{s}$  content of the nucleon than the pionic  $\sigma_{\pi N}$  terms <sup>42)</sup>..

The DEAR Collaboration (a total of 12 Institutes from 6 countries) will take data as soon as the first stable beams circulate in the DAΦNE rings.

## 6 Conclusions

A wealth of physics ranging from CP violation to hypernuclear studies is expected from DAΦNE . Machine commissioning is in progress; construction of the detectors is well underway.

I gratefully acknowledge the help and information given by my colleagues on the

DAΦNE project team, DEAR collaboration, FINUDA collaboration, and KLOE collaboration, particularly G. Vignola, C. Guaraldo, C. Petrascu, F.L. Fabbri, R. Baldini, J. Lee-Franzini, P. Franzini, S. Giovannella and S. Miscetti. I also thank V. Serdiouk for his comments on this manuscript. Finally, I wish to thank the Organizing Committee for a perfectly enjoyable Symposium.

## References

1. Maiani L., et al. (Eds.), *The Second DAΦNE Physics Handbook*, Frascati: SIS Laboratori Nazionali di Frascati (1995).
2. Baldini R., et al. (Eds.), *Proc. II Work. on Phys. and Detector for DAΦNE*, Frascati Physics Series **4**, Frascati: SIS Laboratori Nazionali di Frascati (1996).
3. The Frascati home page is <http://www.lnf.infn.it/>.
4. The  $\phi$ -factory group, *Proposal for a  $\phi$ -factory*, Frascati Report 90/031(R) (1990).
5. The DAΦNE project team, *DAΦNE Machine Project*, Proc. EPAC 94, London, 1994, also Frascati report LNF-94/055(P) (1994).
6. Status Report on DAΦNE, G.Vignola, ref. <sup>2</sup>).
7. Any textbook will discuss the basics of kaon physics. For a clear, elementary level discussion see: Perkins D.H., *Introduction to High Energy Physics*, Addison Wesley (1987).
8. For a more advanced and up-to-date review see: Leader E. and Predazzi P., *An introduction to gauge theories and modern particle physics*, Cambridge Monographs on Particle Physics **4**, Cambridge: Cambridge University Press (1996).
9. M. Gleiser, these Proceedings.
10. R. Peccei, *Proc. 23rd INS Int. Symp. on Nucl. and Part. Phys.*, Tokyo: Univ. Academy Press, Inc., 3 (1995).
11. L. K. Gibbons et al. (E731 Collab.), *Phys. Rev. Lett.* **70**, 1203-1206 (1993).
12. G. D. Barr et al (NA31 Collab.), *Phys. . Lett.* **B317**, 233-242 (1993).
13. G. Buchalla et al., *Nucl. Phys.* **B349**, 1 (1991).
14. S. Bertolucci et al., *Nucl. Phys. B (Proc. Suppl.)* **37A**, 43 (1994).



15. J. Lee-Franzini, *Proc. Heavy Quarks at Fixed Target, St.Goar (Germany), Oct. 3rd, 1996*, Frascati Physics Series **7**, 363, Frascati: SIS Laboratori Nazionali di Frascati (1997).
16. F. Anulli *et al.*, LNF Report 95-007(P) (1995).
17. J. Lee-Franzini, W. Kim, P. J. Franzini, *Phys. Lett.* **B287**, 259 (1992).
18. The KLOE Collaboration, LNF Reports LNF-92/019 (1992), LNF-93/002 (IR) (1993), LNF-94/028 (1994), LNF-95/014 (1995), LNF-96/043 (1996).
19. D. Babusci *et al.*, *Nucl.Instr. and Meth.* **A332**, 444 (1993).
20. A. Antonelli *et al.*, *Nucl. Instr. and Meth.* **A354**, 352 (1995).
21. M. Antonelli *et al.*, *Proc. ICHEP 96* , in press, Warsaw (1996).
22. A. Antonelli *et al.*, *Status of the KLOE Experiment* Frascati report LNF97/033.
23. T. Bressani, *Proc. Work. on Phys. and Detector for DAΦNE* , Frascati, April 9-12 1991, 475 (G. Pancheri Ed.) (1991).
24. T. Bressani, *Non-mesonic Decay of Hypernuclei and the  $\Delta I = 1/2$  Rule*, ref. <sup>1</sup>).
25. F. L. Fabbri, Frascati Report 96/062(R) (1996).
26. A. Olin, *Low-energy K-N Scattering with FINUDA*, ref. <sup>2</sup>).
27. The FINUDA Collaboration (M. Agnello *et al.*), *The  $K_{e2}$  decay with FINUDA at DAFNE* , presented by T. Bressani at the Workshop on K Physics, Orsay, France, May 30-June 4 (1996).
28. The FINUDA Collaboration (M. Agnello *et al.*), LNF Reports LNF-93/021(IR) (1993), LNF-95/024(IR) (1995).
29. S. Bianco, *Proc. 23rd INS Int. Symp. on Nucl. and Part. Physics*, Tokyo: Univ. Academy Press, Inc., 347 (1995). Also a LNF Report LNF-95/028(P) (1995).
30. M. Agnello *et al.*, *Nucl. Instr. and Meth.* **A379**, 411 (1996).
31. L. Benussi *et al.*, *Nucl. Instr. and Methods* **A361**, 180 (1995).
32. T. Hasegawa *et al.*, *Phys. Rev. Lett.* **74**, 224 (1995).

33. A. Zenoni, *Proc. Workshop on Physics and Detectors for DAΦNE, Frascati, Italy (1995)*, Frascati Physics Series **4**, 293, Frascati: SIS Laboratori Nazionali di Frascati (1996), R. Baldini et al. (Eds.).
34. C. Guaraldo, V. Lucherini and C. Petrascu, *How to solve at DAΦNE the kaonic hydrogen puzzle*, ref. <sup>2</sup>).
35. R. Baldini et al. (The DEAR Collaboration), *DAΦNE Exotic Atoms Research (DEAR Proposal)*, LNF Report LNF-95/055(IR) (1995).
36. M. Iwasaki et al., *Phys. Rev. Lett.* **78** (1997) 3067.
37. C. Petrascu et al., *Expanding GEANT code towards low energy (down to 1 keV) and its application in the DEAR (DAΦNE Exotic Atom Research) Monte Carlo Code* (in preparation).
38. C. Guaraldo (for the DEAR Collab.) *presented at the 15th Meeting of the LNF Scientific Committee* Frascati, November 10-11, 1997.
39. W. Kluge, *Rep. Prog. Phys.* **54** (1991) 1251.
40. B. Di Claudio et al., *Lett. Nuovo Cim.* **26** (1979) 555.
41. J. Gasser et al., *Phys. Lett.* **B253** (1991) 252.
42. R. L. Jaffe et al., *Comments Nucl. Part. Phys.* **17** (1987) 163.